

High-pressure densification of amorphous silica

John S. Tse and Dennis D. Klug

Steacie Institute for Molecular Sciences, National Research Council of Canada, Ottawa, Ontario, Canada K1A 0R6

Yvon Le Page

Institute for Environmental Chemistry, National Research Council of Canada, Ottawa, Ontario, Canada K1A 0R6

(Received 16 March 1992)

Molecular-dynamics simulations using a recently proposed two-body potential were employed to study the structure of amorphous SiO_2 at ambient pressure and the densification that occurs at high pressure. The structures obtained at ambient conditions are in good agreement with experiment. The oxygen coordination number about silicon atoms in the network increases from 4 to about 5 in the material taken to 15 GPa and reaches 6 at high pressures. A densification with a volume reduction of about 20% was calculated for samples subjected to pressures of 15 GPa and higher and then recovered at 1 bar. The transformation is primarily driven by the increased stability of the higher Si-O coordination at high pressures. The oxygen coordination number of amorphous SiO_2 is calculated to be about 4.2–4.4 for samples recovered from 15–20 GPa. The calculations suggest that a new crystalline phase is formed at about 100 GPa.

I. INTRODUCTION

Amorphous SiO_2 ($\alpha\text{-SiO}_2$) is an important prototype material for the study of network glasses. The structure and dynamical behavior are not yet fully understood, however. The reason for the incomplete understanding of this material is that it is experimentally difficult to monitor the short-, medium-, and long-range order in disordered materials using the common experimental techniques. Infrared and Raman spectroscopy can yield information about the short-range order and diffraction methods also characterize short-range order, but it is difficult to apply these techniques with high accuracy at elevated pressures or on microscopic samples. To this end, molecular-dynamics (MD) methods have been employed to model the structure of amorphous SiO_2 and to further the understanding of the process of densification in this material.

In the last 15 years, a number of MD and Monte Carlo (MC) studies of amorphous SiO_2 have been reported.^{1–9} The first was by Woodcock, Angell, and Cheeseman,¹ who used an empirical two-body potential to obtain results which were in apparent agreement with experiment at ambient pressure. These calculations and others required the assumption of the correct density and made use of the (N, V, E) or (N, P, H) ensemble. Later investigators indicated a two-body potential, because of the covalent nature of the bonding, is not adequate to give detailed structural properties and that three-body forces are required.^{10,11} These potentials accurately reproduce the structural properties of $\alpha\text{-SiO}_2$ at moderate pressures and provide important insight into the topological changes occurring in the four-coordinated glass. In most cases the three-body potentials used for simulations of amorphous SiO_2 were parametrized only for fourfold oxygen coordination about the Si atoms and therefore were not

appropriate to describe the densification that is observed in this material. Very recently, two two-body potentials based on quantum mechanical calculations have been proposed which were shown to quite adequately describe both the four- and six-coordinated structures in polymorphic forms of SiO_2 .^{12,13} In particular, the potential of van Beest, Kramer, and van Santen has been used to obtain the structural changes in α -quartz and to yield the mechanism for pressure-induced amorphization.¹⁴ This advance has stimulated several recent studies on the structure and dynamics of SiO_2 at ambient and high pressure.^{15–23} An outstanding problem is that of the amorphous form of SiO_2 , where a densification has been observed and the dense amorphous material can be recovered at ambient pressure. This is analogous in some respects to the densification that has been observed in amorphous ice, which can be prepared by pressurizing the material made by vapor deposition of water or annealing of high-density amorphous ice.^{24,25} In view of the successes in the application of MD methods to the mechanism for pressure-induced amorphization of α -quartz and ice²⁶ using two-body potentials, the densification of $\alpha\text{-SiO}_2$ has been examined with the goal of obtaining an understanding of this phenomenon at the atomic level. Recently, the structure of a recovered densified $\alpha\text{-SiO}_2$ has been studied by both MD calculations and neutron diffraction.²⁷ However, the MD calculations were performed on an amorphous structure obtained by quenching a high-density melt from 3000 K. It should also be noted that have been several other important MD and MC studies on the structure and dynamics of $\alpha\text{-SiO}_2$ (Refs. 11 and 20–23) at high pressure. These studies did not deal specifically with the densification process and the structures of the recovered phase as a function of applied pressure which are the main points addressed in this study.

II. COMPUTATIONAL METHODS

Molecular-dynamics simulations were performed on a model system containing 216 SiO₂ units. The potential used is due to van Beest, Kramer, and van Santen¹³ and is of the form

$$\Phi_{ij} = q_i q_j / r_{ij} + A_{ij} \exp(-b_{ij} r_{ij}) - c_{ij} / r_{ij}^6,$$

where q_i and q_j are the atomic charges, r_{ij} the interatomic distance, and A_{ij} , b_{ij} , and c_{ij} are the force-field parameters. The Nosé isothermal-isobaric ensemble was used for the calculation of the equation of state.^{28,29} Integration time steps of 1-1.5 fs were used and the long-range electrostatic interactions were calculated using the Ewald method.³⁰ Amorphous SiO₂ was prepared by first melting an equilibrated α -cristobalite sample at 7000 K.³¹ The sample was then cooled successively for 4 ps at 3000, 1000, 600, and finally to 300 K to yield an annealed amorphous structure. The amorphous phases obtained at ambient and higher pressures and 300 K were each annealed for 5–40 ps. The x-ray-diffraction patterns were calculated at each pressure from the density operator and the coherent part of the structure factor. The atom-atom radial distribution functions (RDF) and the distribution of near-neighbor Si-O-Si and O-Si-O angles were also calculated.

III. RESULTS AND DISCUSSION

A summary of the computational results is presented as the pressure-volume equation of state (P - V EOS) and compared with the experimental results^{32–34} in Fig. 1. The two-body effective potential employed here gives very reasonable agreement with static pressure measurements from 0 to 15 GPa. The discrepancy is somewhat larger at pressures greater than 20 GPa where the experimental results are obtained from less accurate shock wave data. More significantly, the densification calculated at 15–17 GPa is consistent with the observed discontinuity in the experimental P - V curve. As will be discussed later, the calculated structures of pressurized α -SiO₂ are also in good accord with experiment. Before embarking on the discussion of the densification process, it is important to evaluate the performance of the potential model in reproducing the structure of α -SiO₂ under ambient conditions.

A. α -SiO₂ at ambient pressure

The calculated density of α -SiO₂ at 1 bar and 300 K from the potential model of van Beest, Kramer, and van Santen is 2.36 g/cm³ which is about 7% higher than the observed value.³⁵ The present value is among the best obtained from first-principles MD or MC calculations. A recent constant pressure-constant temperature (NPT) MD calculation³¹ using an empirical three-body potential gave a density of 2.92 g/cm³ at 300 K. On the other hand, a recent MC calculation¹¹ using another three-body potential gave a result comparable to that of the present study. In spite of the success of the three-body potential in giving correct densities at low pressures, this potential is not applicable for high pressures since it is

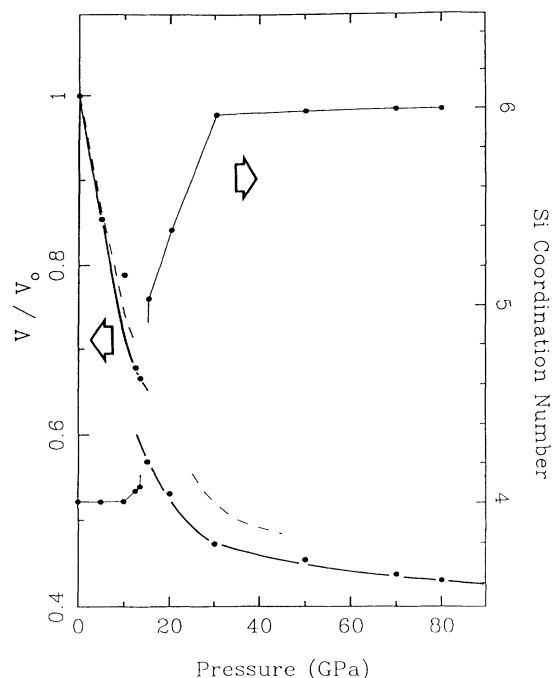


FIG. 1. Calculated (solid line) and measured (dashed line) volume reduction and the Si-O coordination number of amorphous SiO₂ vs pressure at 300 K. The experimental volumes for pressures up to 12 GPa are the results of static pressure experiments (Refs. 32 and 33). The experimental volumes for higher pressures are from shock wave data (Ref. 34).

parametrized specifically for four-coordinated silica units. The three-body potential failed to reproduce the densification of α -SiO₂ at about 15 GPa. In order to make a direct comparison of structure obtained by the simulation with that of the experiment, it is more appropriate to compare the x-ray-diffraction patterns rather than the customary atomic radial distributions, which are derived from the experimental diffraction pattern subject to several assumptions. The x-ray-diffraction pattern of α -SiO₂ at 1 bar and 300 K is shown in Fig. 2 and compared with experiment.³⁵ The agreement is very satisfactory. The calculated diffraction pattern is typical of that of an amorphous solid having a broad distribution of scattering intensity. In particular, the weak features observed at about 6.5, 8.5, and 12.5 Å⁻¹ are well reproduced by the calculation, indicating that both the long- and short-range order are well represented by the two-body potential. The atomic radial distribution functions obtained from the calculations are shown in Fig. 3. The nearest-neighbor Si-O, O···O, and Si···Si distances are 1.60(1), 2.61(1), and 3.11(1) Å, respectively, which are in excellent agreement with experiment.³⁶

The bond-angle distribution for the Si-O-Si and O-Si-O nearest-neighbor angles calculated with a Si-O cutoff distance of 2.0 Å are shown in Fig. 4. At 1 bar the Si-O-Si bond-angle distribution extends from about 120 to 180° with a maximum at about 142° and a distinct broad shoulder at 157°. Since the chemical shift of the ²⁹Si nucleus is sensitive to the local environment, a distribution of the Si-O-Si angle can be derived directly from the

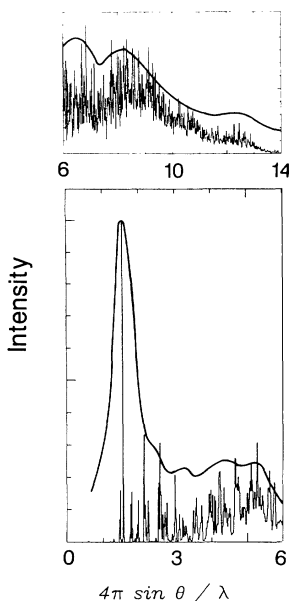


FIG. 2. Calculated and measured (Ref. 35) x-ray-diffraction pattern of amorphous SiO_2 at 1 bar and 300 K.

analysis of the solid-state ^{29}Si line shape.³⁷ The calculated distribution of the Si-O-Si angle is in substantial agreement with the NMR results, which also show a bimodal distribution. It is noteworthy that a similar angular distribution has not been reported in previously published calculations on $\alpha\text{-SiO}_2$. At 1 bar, the calculated Si-O-Si bond-angle distribution is considerably broader than that calculated for $\alpha\text{-quartz}$. The half width is almost three times larger in the amorphous solid. In contrast, the calculated O-Si-O angle distribution is nearly a single peak similar to that of $\alpha\text{-quartz}$ except that in $\alpha\text{-quartz}$ there is a distinct skew at high angles. The distribution maximum is at the ideal tetrahedral angle of 109.5° and it is only slightly broader in the amorphous phase. This observation suggests that the SiO_4 tetrahedra in the amorphous solid are not severely distorted at 1 bar and that the disorder in $\alpha\text{-SiO}_2$ is a result of a large distribution of intertetrahedral angles. The calculated density of vibra-

tional states supports this observation in that the maxima in the region dominated by internal vibrations of Si atoms in tetrahedral units occur in the same frequency regions as in $\alpha\text{-quartz}$ and are only broadened slightly.

B. $\alpha\text{-SiO}_2$ at high pressures

The calculated density of $\alpha\text{-SiO}_2$ at elevated pressures is compared with experimental data in Fig. 1. The good agreement between the calculated and observed density at elevated pressures indicates that the two-body potential used is a substantial improvement over previously tested potentials. The calculated densities at low pressure (< 15 GPa) are generally less than the observed values by 5–7%. A densification is predicted at the pressure range 15–20 GPa and this will be discussed in detail in the next section.

At even higher pressures > 100 GPa, the features in the atomic RDF's sharpen considerably (Fig. 3). At 140 GPa, the distribution of nearest-neighbor Si-O-Si and O-Si-O angles also sharpens (Fig. 4) and the calculated x-ray-diffraction pattern resembles that of a crystalline solid. A block of atoms at the center of the simulation box was selected to identify the translationally equivalent units. The solid phase stable at 140 GPa could be identified as monoclinic $I2/a$ with cell parameters $a=4.24$, $b=4.60$, and $c=11.70$ Å with $\beta=99.9^\circ$. Upon decreasing the pressure to 80 GPa, this phase reverts back to the amorphous phase, indicating that the crystalline phase is nonquenchable. The conversion of the crystalline form to an amorphous form by decompression may be analogous to decompression melting observed in other silicates³⁸ and high-pressure phases of ice.³⁹ The high-pressure phase is not recoverable, in agreement with the experimental findings of Tsuchida and Yagi⁴⁰ for a post-stishovite phase of SiO_2 .

To obtain a better estimate of the cell parameters and total energy of the new monoclinic phase, a separate calculation employing 384 SiO_2 units starting with the idealized structure obtained as described above was performed at 140 GPa. The $I2/a$ structure remained stable. In comparison with the other structures which have been

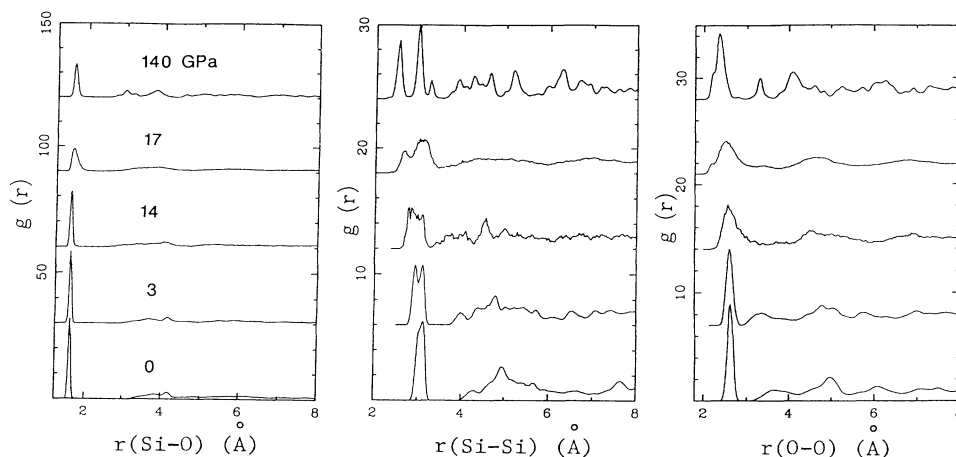


FIG. 3. Calculated atomic radial distribution functions of amorphous SiO_2 at several pressures at 300 K.

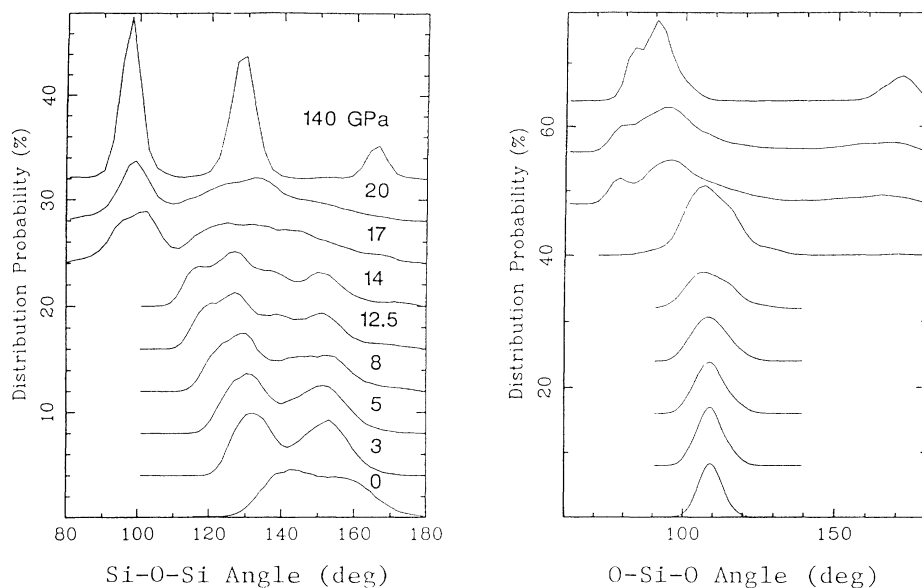


FIG. 4. Calculated bond-angle distributions for the nearest-neighbor Si-O-Si and O-Si-O bond angles in amorphous SiO₂ at various pressures and 300 K.

suggested to be stable in this region, such as the rutile (stishovite), or the cubic phase,⁴¹ the energy of the monoclinic structure is found to be competitive with the rutile structure and is much more favorable than that of the cubic phase. It should be noted that the alternative CaCl₂ structure is not calculated to be stable below 250 GPa.⁴⁰ A post-stishovite phase of SiO₂ has been observed experimentally by x-ray diffraction at 120 GPa and the structure was identified as CaCl₂ from only four observed diffraction lines.⁴² Incidentally, these diffraction lines are also consistent with the novel monoclinic structure found here by MD calculations. More theoretical and experimental work is now needed to establish the physical existence of this calculated new phase.

C. Mechanism of densification

The analysis of the bond-angle distributions and atomic RDF's will give a clear picture of the densification process in *a*-SiO₂. For this purpose a series of calculations by compressing *a*-SiO₂ gradually to 20 GPa and then releasing the pressure in steps to 1 bar were performed. The densification is calculated to take place over the pressure range 15–20 GPa. The onset of densification at 15 GPa is accompanied by an increase in the oxygen coordination around the silicon atoms. The oxygen coordination within a sphere defined by a Si-O distance of 2.5 Å from a silicon atom (Fig. 1), remains at 4 up to about 14 GPa and then increases to about 5 at 15 GPa and rapidly to 6 by 20 GPa. The atom-atom RDF's in Fig. 3 show that by 17 GPa the Si-Si RDF has broadened greatly. The average number of Si atoms within a coordination radius of 3.5 Å increases from 4 at 1 bar to about 7 at 17 GPa. The nearest-neighbor Si-O distances increase slightly over the same pressure range from 1.60 to 1.63 Å as the oxygen coordination increases to 5. The first peak in the O-O atomic RDF integrated to 3.0 Å gives six

neighbors at 1 bar and about ten at 17 GPa. On the other hand, the O-Si-O bond-angle distributions (Fig. 4) broaden considerably as the pressure is increased with the half widths reaching 18° and 27° at 14 and 17 GPa, respectively, with a concomitant decrease in the mean O-Si-O angle by about 12°.

There are several similarities and distinct differences between the effect of pressure on the structures of *a*-SiO₂ and α -quartz. The distribution of the O-Si-O angles in *a*-SiO₂ for pressures up to 14 GPa closely resembles that found in α -quartz indicating that, upon compression up to 14 GPa, the distortion of the SiO₄ polyhedra occurs in a similar manner.¹⁴ The densification in *a*-SiO₂ above 15 GPa is accompanied by a large downward shift in the O-Si-O angle distribution to yield two broad distributions at 80 and 95° by 17 GPa. After the densification a distinct peak begins to develop at about 165°, where oxygen atoms from neighboring SiO₄ tetrahedra begin to participate in edge sharing. This is in accord with the calculated increase in the average coordination number from 4 to about 5 from 14 to 17 GPa. In comparison, in α -quartz the O-Si-O angle distribution continues to broaden beyond 14 GPa and eventually develops into two distinct peaks at 103 and 115° immediately before its calculated phase transition at 22 GPa. The reason is that in α -quartz, the crystalline structure is maintained up to the transformation. In contrast, the structure of *a*-SiO₂ changes gradually from 15 to 20 GPa with increasing oxygen coordination over this range. The Si-O-Si bond-angle distribution in *a*-SiO₂ shows significant changes with increasing pressure, the distribution shifts to lower angles, and a distinct shoulder develops at about 118° by 14 GPa which becomes a dominant peak at about 100° by 17 GPa. On the other hand, the Si-O-Si distribution in α -quartz remains as a single peak up to its phase transition at 22 GPa. This difference in behavior emphasizes the fact that the already quite disordered packing of SiO₄

tetrahedra evolves more easily to a denser amorphous material in α -SiO₂ with the application of pressure. Above 30 GPa to the highest pressure studied here (140 GPa), α -SiO₂ is calculated to remain 6 coordinated. The structural description of α -SiO₂ obtained from the present calculations above the pressure range where densification occurs are consistent with an earlier analysis using Voronoi polyhedra. The earlier results also showed that octahedra are the most abundant species between 30 and 135 GPa.²¹ It should be emphasized that the comparison is not entirely appropriate since the previous calculations were performed at substantially higher temperature and therefore should reflect a more liquidlike behavior.

D. α -SiO₂ recovered from high pressures

It is found that α -SiO₂ compresses elastically when the pressure is below 14 GPa, that is, the ambient pressure structure is recovered once the pressure is relieved. Above 15 GPa, a densified structure is maintained. When the pressure was removed on samples taken to 14, 15, 17, and 20 GPa, the ratio of the densities of the recovered samples to that of the initial density at 1 bar of each sample after 4 ps of annealing at 300 K and 1 bar were 0.99, 0.80, 0.76, and 0.74, respectively. The recovered densified structures obtained from the calculations may not be fully relaxed within the time scale of the simulation. To investigate this possibility a sample that was pressurized to 17 GPa and recovered at 1 bar was allowed to anneal at 300 K for an additional 40 ps, and the density was found to decrease gradually further by 1%. Nonetheless, the volume reduction of the recovered densified α -SiO₂ at 20 GPa of 20% is consistent with the 18–20% observed experimentally.⁴³ The coordination number of the material recovered at 1 bar was about 4.2–4.4 for samples recovered from 15–20 GPa. This is in good agreement with experiment, which shows no significant change in coordination number.³⁶ The bond-

angle distribution for Si-O-Si and O-Si-O angles differs significantly from that of the starting material (Fig. 5) when the applied pressure is 15 GPa or greater. In particular, the broad distribution of O-Si-O angles is retained, indicating that the SiO₄ tetrahedra remain highly distorted in the densified material. The maximum in this distribution moves upward by about 14° almost to the tetrahedral angle indicating considerable recovery of many of the SiO₄ tetrahedra. The Si-O-Si angle distribution retains the shoulder at about 100° which is a remnant of the edge-sharing feature characteristic of the high-pressure structure. The small shoulder that remains in the O-Si-O angle distribution also reflects the fact that some features of a five- or higher coordinated structure are being retained.

The MD calculations reported here are for densification at room temperature and therefore can be compared directly with the recent neutron-diffraction results of Susman *et al.*²⁷ on samples that had been compressed at room temperature to 16 GPa. The reported densification of 20% is in excellent agreement with that reported here. In addition there are several features of the RDF's which indicate the potential used here is quite reliable. The first maximum in the O-O RDF of the material recovered from 17 GPa is substantially higher than that for the starting material with the half width [full width at half maximum (FWHM)] broadened by about 0.1 Å. These observations are in substantial agreement with the experimental weighted pair correlation function. The small peaks calculated at ca. 90° in both the O-Si-O and Si-O-Si distribution (Fig. 5), which reflect the retention of some higher coordination features, are not present in the previous MD calculations on the quenched melt. This discrepancy is probably due to the fact that the structure obtained from quenching of a densified liquid is not a good representation of the disordered structure obtained by pressurization. Previous experimental and theoretical studies on the pressure-

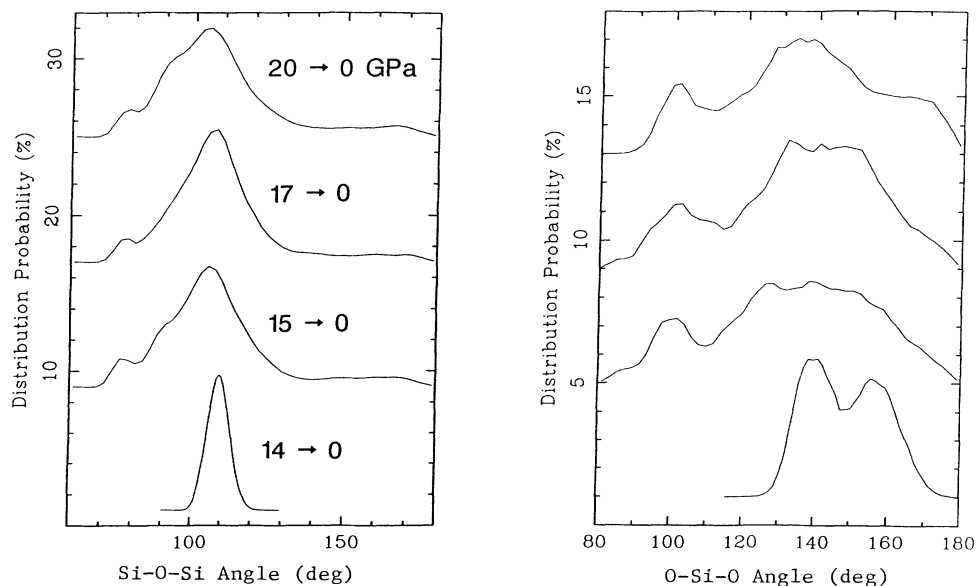


FIG. 5. Calculated bond-angle distribution for the nearest-neighbor angles in samples recovered from 14, 15, 17, and 20 GPa.

induced transformation in ice,⁴⁵ α -quartz,⁴⁶ and α -berlinite⁴⁷ have clearly shown that the densified structures do not resemble that of the corresponding dense liquids.

There are several features of the pressure-induced densification of a -SiO₂ which appear to be found in other materials such as ice.⁴⁴ The densification occurs with an increase in coordination number and with an elongation of near-neighbor bond lengths. The densified material can be recovered at ambient pressure. In addition, the densification of a -SiO₂ occurs at significantly lower pressures than is observed in α -quartz. This is analogous to the behavior found in low-density amorphous ice prepared by vapor deposition or by annealing high-density amorphous ice. It undergoes densification at significantly lower pressures than crystalline ice. It should be emphasized that the amorphous forms made with different methods did not have the same structures.

In ice the densities differed by about 10% at pressures just after densification. Although there are no similar measurements for SiO₂, the calculated radial distribution functions differ significantly.

In summary, classical MD calculations using a two-body potential obtained from a quantum calculation of a cluster and then optimized with empirical data for crystalline phases of quartz show the observed densification of amorphous quartz and yield a detailed picture at the atomic level of this phenomenon. In addition, a metastable monoclinic crystalline form is predicted to occur at pressures near 1 Mbar. Further theoretical and experimental work is required to verify this result. These results suggest that MD methods with accurate two-body potentials should be an increasingly important tool for the study of densification and order⁴⁷ in amorphous solids.

- ¹L. V. Woodcock, C. A. Angell, and P. Cheeseman, *J. Chem. Phys.* **65**, 1565 (1976).
- ²S. K. Mitra and R. W. Hockney, *J. Phys. C* **13**, L739 (1980).
- ³T. F. Soules, *J. Chem. Phys.* **71**, 4530 (1979).
- ⁴C. A. Angell, P. A. Cheeseman, and C. C. Phifer, in *Materials Research Society Symposium Proceedings* (Materials Research Society, Pittsburgh, 1985), Vol. 63, p. 85.
- ⁵S. K. Mitra, M. Amini, and D. Fincham, *Philos. Mag. B* **43**, 365 (1981).
- ⁶S. K. Mitra and J. M. Parker, *Phys. Chem. Glasses* **25**, 95 (1984).
- ⁷B. Vessal, M. Leslie, and C. R. A. Catlow, *Mol. Simulat.* **3**, 123 (1989).
- ⁸B. P. Feuston and S. H. Garafalini, *J. Chem. Phys.* **89**, 5818 (1988).
- ⁹J. D. Kubicki and A. G. Lasaga, *Am. Mineral.* **73**, 941 (1988).
- ¹⁰J. R. Chelikowsky, H. E. King, Jr., N. Troullier, J. L. Martins, and J. Glinnemann, *Phys. Rev. Lett.* **65**, 3309 (1990); J. R. Chelikowsky, H. E. King, Jr., and J. Glinnemann, *Phys. Rev. B* **41**, 10866 (1990).
- ¹¹L. Stixrude and M. S. T. Bukowinski, *Phys. Rev. B* **44**, 2523 (1991).
- ¹²S. Tsuneyuki, M. Tsukada, H. Aoki, and Y. Matsui, *Phys. Rev. Lett.* **61**, 869 (1988).
- ¹³B. W. H. van Beest, G. J. Kramer, and R. A. van Santen, *Phys. Rev. Lett.* **64**, 1955 (1990).
- ¹⁴J. S. Tse and D. D. Klug, *Phys. Rev. Lett.* **67**, 3559 (1991).
- ¹⁵J. S. Tse and D. D. Klug, *J. Chem. Phys.* **95**, 9176 (1991).
- ¹⁶S. Tsuneyuki, Y. Matsui, H. Aoki, and M. Tsukada, *Nature (London)* **339**, 209 (1989).
- ¹⁷S. Tsuneyuki, H. Aoki, and Y. Matsui, *Mol. Simulat.* **6**, 227 (1991).
- ¹⁸S. Tsuneyuki, H. Aoki, M. Tsukada, and Y. Matsui, *Phys. Rev. Lett.* **64**, 776 (1990).
- ¹⁹Y. Matsui and S. Tsuneyuki, in *High Pressure Research: Application to Earth and Planetary Sciences*, edited by Y. Syono and M. H. Manghni: (Terra Scientific Publishing Co., Tokyo/American Geophysical Union, Washington, D.C.), to be published.
- ²⁰J. R. Rustad, D. A. Yuen, and F. Spera, *Phys. Rev. B* **42**, 2081 (1990).
- ²¹J. R. Rustad, D. A. Yuen, and F. Spera, *Phys. Rev. B* **44**, 2108 (1991).
- ²²J. R. Rustad, D. A. Yuen, and F. Spera, *J. Geophys. Res.* **96**, 19665 (1991).
- ²³J. R. Rustad, D. A. Yuen, and F. Spera, *Phys. Earth Planet. Inter.* **65**, 210 (1991).
- ²⁴O. Mishima, L. D. Calvert, and E. Whalley, *Nature (London)* **314**, 76 (1985).
- ²⁵M. A. Floriano, Y. P. Handa, D. D. Klug, and E. Whalley, *J. Chem. Phys.* **91**, 7187 (1989).
- ²⁶J. S. Tse and M. L. Klein, *Phys. Rev. Lett.* **58**, 1672 (1987).
- ²⁷S. Susman, K. J. Volin, D. L. Price, M. Grimsditch, J. P. Rino, R. K. Kalia, and P. Vashishta, *Phys. Rev. B* **43**, 1194 (1991).
- ²⁸S. Nosé, *J. Chem. Phys.* **81**, 511 (1984).
- ²⁹S. Nosé and M. L. Klein, *Mol. Phys.* **50**, 1055 (1983).
- ³⁰P. Ewald, *Ann. Phys. (N.Y.)* **64**, 253 (1921).
- ³¹B. Vessal, M. Amini, D. Fincham, and C. R. A. Catlow, *Philos. Mag. B* **60**, 753 (1989).
- ³²P. W. Bridgman, *Proc. Am. Acad. Arts Sci.* **76**, 55 (1948).
- ³³C. Meade and R. Jeanloz, *Phys. Rev. B* **35**, 236 (1987).
- ³⁴S. P. Marsh (unpublished).
- ³⁵R. L. Mossi and B. E. Warren, *J. Appl. Crystallogr.* **2**, 164 (1969).
- ³⁶P. McMillan, B. Piriou, and R. Coty, *J. Chem. Phys.* **81**, 4234 (1984).
- ³⁷L. F. Gladden, T. A. Carpenter, and S. R. Elliot, *Philos. Mag. B* **53**, L81 (1986).
- ³⁸P. Richet, *Nature (London)* **331**, 56 (1988).
- ³⁹D. D. Klug, Y. P. Handa, J. S. Tse, and E. Whalley, *J. Chem. Phys.* **90**, 2390 (1989).
- ⁴⁰Y. Tsuchida and T. Yagi, *Nature (London)* **347**, 267 (1990).
- ⁴¹K. T. Park, F. Terakura, and Y. Matsui, *Nature (London)* **336**, 670 (1988).
- ⁴²Y. Tsuchida and T. Yagi, *Nature (London)* **340**, 217 (1989).
- ⁴³A. Polian and M. Grimsditch, *Phys. Rev. B* **41**, 6086 (1990), and references cited therein.
- ⁴⁴D. D. Klug, O. Mishima, and E. Whalley, *J. Chem. Phys.* **86**, 5323 (1987).
- ⁴⁵J. S. Tse, *J. Chem. Phys.* **96**, 5482 (1992).
- ⁴⁶L. E. McNeil and M. Grimsditch, *Phys. Rev. Lett.* **68**, 83 (1992).
- ⁴⁷J. S. Tse and D. D. Klug, *Science* **255**, 1559 (1992).